Abdominal Radiology (2019) 44:3874–3885
https://doi.org/10.1007/s00261-019-02173-2

SPECIAL SECTION : UROTHELIAL DISEASE

Upper urinary tract urothelial carcinoma on multidetector CT: spectrum of disease

Osama Ali[1] · **Elliot K. Fishman**[1] · **Sheila Sheth**[1]

Published online: 9 November 2019

Abstract
Urothelial carcinoma of the upper urinary tract (UUT) is a relatively uncommon genitourinary malignancy, accounting for about 5–7% of urothelial tumors. The significant features of this tumor are multifocality and high rate of recurrence. Computed tomography urography (CTU) has replaced excretory urography (EU) and retrograde pyelography (RP) for imaging of upper tract urothelial carcinoma. While many studies have confirmed high sensitivity (88–100%) and specificity (93–100%) of CTU, an optimized CT protocol is of critical importance in screening, staging, and post-operative follow-up of patients (Chlapoutakis, Eur J Radiol 73(2):334–338, 2010; Caoli and Cohan, Abdom Radiol (NY) 41(6):1100–1107, 2016). The key element of the CT protocol is to have adequate distension of the collecting system with excreted contrast, to detect subtle lesions at an early stage. In this article, we discuss the background of upper urinary tract TTC, pathogenesis, CT protocol and the role of imaging in evaluation of this malignancy, staging, as well as different imaging appearances.

Introduction

Urothelial carcinoma of the upper urinary tract (renal collecting system and ureter) is a relatively uncommon malignancy, accounting for 5–7% of urothelial tumors [3] and up to 10–15% of all renal tumors [2]. The exact incidence of upper urinary tract urothelial carcinoma is difficult to assess, given its rarity; about 2290 Americans were diagnosed with ureteral urothelial carcinoma, and nearly 700 patients died from it in 2008 [4]. The renal pelvis is the most commonly involved site in the UUT [3], and is second to the urinary bladder in overall incidence of urothelial carcinoma [4].

When the ureter is affected, the most commonly involved segment is the distal third (73%), followed by the mid ureter (24%), and proximal ureter (3%). Bilateral ureteral involvement occurs in 2–5% of cases [2]. Approximately, 11–13% of patients with upper tract urothelial carcinoma develop metachronous upper tract tumors [5]. Patients usually present with microscopic or gross hematuria, flank pain, or renal colic. However, up to 20% of lesions are detected incidentally or during surveillance imaging for a known urothelial tumor in the urinary bladder [2, 3].

Multifocality is a key feature in urothelial carcinoma warranting long-term surveillance. Up to 40% of patients with UUT urothelial carcinoma will develop a metachronous tumor in the urinary bladder, usually within the first 2 years following surgical resection, and this is typically seen more with ureteric tumors than with renal pelvic tumors. Approximately, 2–9% of patients with urothelial carcinoma of the urinary bladder have a metachronous upper tract urothelial carcinoma [2–5].

Etiology and Pathologic Features

The most important risk factors for UUT urothelial carcinoma are male gender, age above 60 years, and tobacco use. Chemical carcinogens excreted in the urine such as benzidine or aniline dyes, cyclophosphamide, phenacetin-based analgesics, and chronic urinary tract infections are also predisposing factors [3]. Patients with hereditary non-polyposis colon cancer (Lynch syndrome) have a higher incidence of urothelial cancer. Balkan nephropathy, a form of interstitial nephritis, endemic in Eastern Europe poses a higher risk for development of urothelial carcinoma. The incidence of upper urinary tract urothelial carcinoma in this region is estimated to be 100 times higher than in non-endemic regions [6].

✉ Osama Ali
Oali4@jhmi.edu

[1] Russell H. Morgan Department of Radiology and Radiological Science, Johns Hopkins School of Medicine, Johns Hopkins University, 601 N. Caroline Street/JHOC 3235A, Baltimore, MD 21287, USA

These patients tend to have familial metabolic aberrations, and along with environmental exposure to organic toxins, the kidneys are exposed to a persistent influx of toxins that increases the risk for subsequent development of urothelial carcinomas [3].

Papillary forms of urothelial carcinoma in the upper urinary tract, which accounts for up to 85% of urothelial carcinomas, are cytologically and histologically similar to their urinary bladder counterpart [5, 7]. These tumors are usually low-stage and superficial, with frondlike morphology, and tend to have a slow growth rate with a relatively indolent course [5]. Solid, flat tumors, accounting for approximately 15% of cases, tend to be more aggressive with a higher stage at presentation [5, 7].

Imaging of UUT urothelial carcinoma

CTU has largely replaced conventional modalities, such as excretory urography and retrograde pyelogram, in evaluation of UUT urothelial carcinoma in recent decades. Both the American College of Radiology 2014 appropriateness criteria and the American Urological Association 2012 guidelines [8] recognize that CTU is now considered the imaging modality of choice in evaluation of adult patients presenting with microscopic or macroscopic hematuria, given its high specificity and relatively high sensitivity [9, 10]. Chlapoutakis et al. [1] conducted a meta-analysis to estimate the sensitivity and specificity of CTU in detection of urothelial malignancy; it was concluded that CTU has a pooled sensitivity and specificity of 88–100% and 93–100%, respectively. However, benign entities can create a diagnostic dilemma. Sadow et al. [11] reported a 53% overall positive predictive value of CTU in detection of urothelial malignancy, and 83% for large masses.

CT protocol

An optimized CTU protocol is crucial in evaluation of patients suspected to have urothelial malignancy or other etiologies for hematuria. The main goal is to maximize distension and opacification of the collecting system, to increase sensitivity for detection of subtle abnormalities.

Timing of contrast injection

Different CT protocols have been proposed, including single bolus, split bolus, and triple bolus techniques.

The most widely used is a single bolus technique, where a single bolus of intravenous contrast (roughly 120 mL) is injected, followed by acquisition of dynamic imaging in the arterial (corticomedullary), nephrographic, and excretory phases. The two main advantages of this technique include simplicity for the technologists and maximal distension of the collecting system since the entire bolus of contrast is used for parenchymal opacification of the collecting system. However, the trade-off is increased radiation dose (multiple acquisitions are obtained). Addition of a fourth phase to this technique, non-contrast imaging prior to injection of intravenous contrast, varies among institutions; non-contrast images allows for increasing sensitivity for detection of small stones in the upper urinary tract and assessment of enhancement of renal/ureteral soft tissue lesions. Newer scanner technologies, such as creation of virtual non-contrast images (substituting acquisition of non-contrast images) offer some promise in reducing radiation dose to patients [2, 12–15].

In the split bolus technique, two separate injections of intravenous contrast are administered. Initially, about 50–100 mL of contrast are injected, followed by a 5-minute delay, and then another injection of about 40–80 mL. The patient is then imaged at 7 min [2, 12]. Utilizing this technique, the first bolus will be already excreted into the collecting systems and ureters at the time of imaging and the second bolus provides opacification of the renal parenchyma, thus allowing acquisition of a combined nephrographic/excretory phase [2, 12]. The main advantage of this technique is the reduced radiation dose since the number of acquisitions needed is reduced. On the other hand, comparison between single bolus and split bolus techniques has shown inferior collecting system distension in the latter [16] with potentially reduced sensitivity for detection of subtle lesions [2, 12, 16, 17]. Other disadvantages include decreased sensitivity for detection of subtle RCCs as well as inadequate staging and preoperative planning should a malignant lesion be present, since only one or two post-contrast phases are obtained in contrast to three phases in the single bolus technique [12].

Least popular, the triple bolus technique involves splitting the total contrast dose into three separate injections, and subsequently a single acquisition is obtained combining corticomedullary, nephrographic, and excretory phases. Although the total radiation dose is significantly reduced utilizing this technique, distension of the collecting systems and ureters as well as detection of subtle RCCs is a major concern, as with the split bolus technique [2, 12].

Techniques to maximize distension of the collecting system

Additional techniques, aiming to improve distension of the collecting systems and ureters, have been described in the literature. These include abdominal compression, use of diuretics, oral or intravenous hydration, and log-rolling [2, 12]. The two techniques with most supporting data are

the use of low-dose diuretics and oral/intravenous hydration [12, 18].

The administration of diuretics (typically 10–20 mg of Furosemide IV for 2–3 min prior to injection of contrast) has been shown to improve distension of the collecting systems and ureters, and achieve the best opacification of the mid and distal ureter [19]. It also dilutes excreted contrast in the collecting system, lessening beam-hardening artifacts from dense contrast [19, 20]. However, diuretics administration comes at the cost of delaying the work flow, especially at a busy practice, requires nursing expertise for administration, and checking for potential contraindications and cross-reactions with other medications [12]. Hydration has been proven in the literature to successfully allow optimal distension of the collecting systems, particularly the distal ureters and dilution of excreted contrast, with no adverse impact on workflow. Intravenous (100–250 mL of saline) or oral hydration (roughly 500–1000 mL) can be used, typically given just before the study [18, 21–23].

Other ancillary techniques, such as abdominal compression and prone imaging have also been proposed; however, there is no strong evidence in the literature supporting their benefit.

In summary, a number of CTU protocols have been proposed in the literature, all involving trade-offs between ease of implementation, workflow, radiation dose and optimal image quality. We believe our patients are best served if we maximize detection and characterization of all urological malignancies and avoid inconclusive studies or repeat imaging. At our institution, we use a single bolus technique with a total of four acquisitions in patients above 35 years of age and pre-imaging oral hydration. Non-contrast imaging is followed by an injection of approximately 120 mL

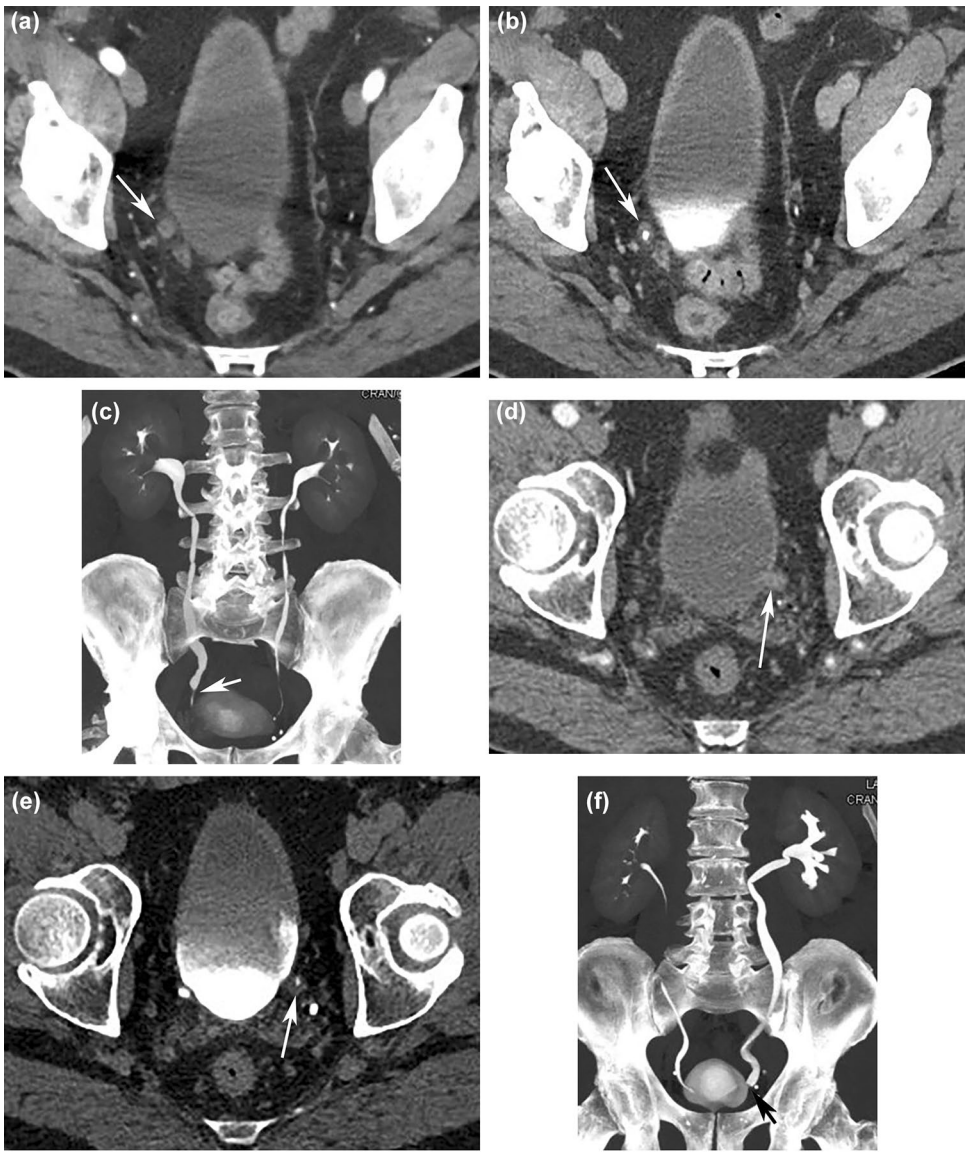

Fig. 1 Urothelial carcinoma with urothelial thickening in the ureter. 63-year-old male with right ureter urothelial carcinoma. **a** Axial CT image of the pelvis in the arterial phase shows circumferential wall thickening of the distal right ureter (white arrow). **b** Axial CT image of the pelvis in the excretory phase better delineates the circumferential wall thickening of the distal ureter (white arrow). **c** Coronal MIP image of the abdomen and pelvis in the excretory phase shows abrupt change in caliber of the distal right ureter (white arrow). Note the increased distension in the right collecting system and ureter compared to the left side, which is an indirect sign that draws attention to the presence of an obstructing lesion. 64-year-old male with urothelial carcinoma in the left ureter. **d** Axial CT image of the pelvis in the arterial phase shows enhancing soft tissue lesion in the left ureter at the ureterovesical junction (white arrow). **e** Axial CT image in the excretory phase, at a level just proximal to (**d**), shows asymmetric urothelial thickening in the distal left ureter (white arrow). **f** Coronal MIP image in the excretory phase shows abrupt transition in the distal left ureter (black arrow), secondary to obstruction by the lesion shown in (**d**). Note the resultant upstream hydroureteronephrosis

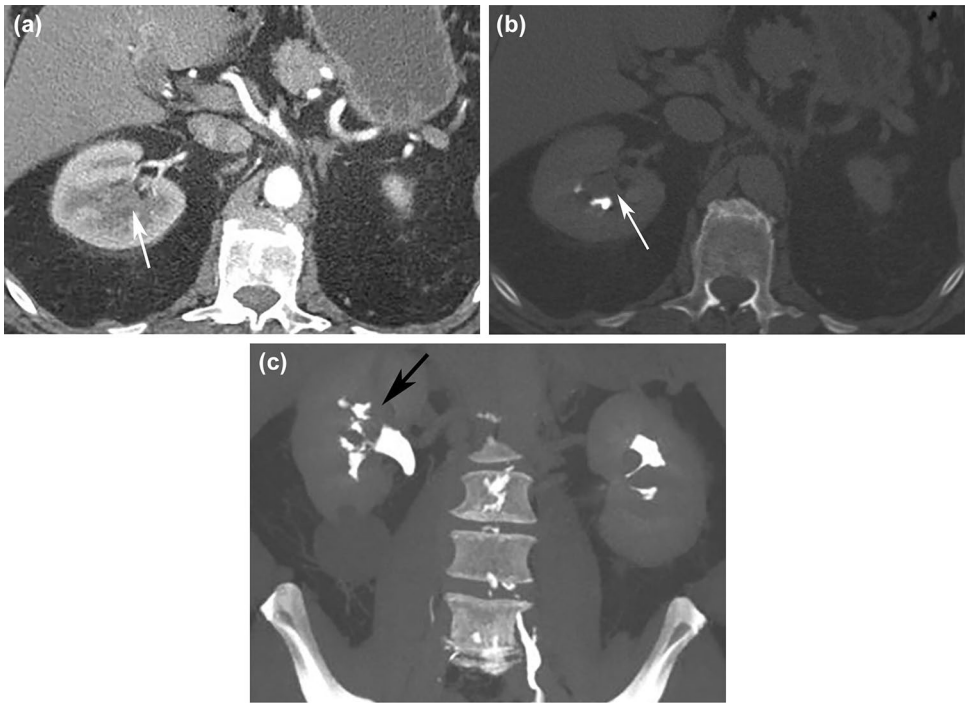

Fig. 2 Upper pole calyx urothelial carcinoma. 67-year-old male with upper pole calyx urothelial carcinoma. **a** Axial CT image of the abdomen at the level of the right kidney in the arterial phase shows very subtle soft tissue thickening in the upper pole calyx (white arrow). **b** Axial excretory phase image (wide window setting) allows for better visualization of a filling defect in the calyx (white arrow), consistent with urothelial carcinoma. The subtle soft tissue thickening in the upper pole calyx on arterial phase images (**a**) is much easier to detect following evaluation of the excretory phase images (**b**). Note obliteration of the upper pole calyx infundibulum on coronal excretory phase image utilizing MIP technique (**c**)

of Omnipaque 350 mg/mL (GE Healthcare); arterial phase imaging is obtained using bolus tracking (region of interest in the abdominal aorta), followed by nephrographic and excretory phases at a fixed delay (50–60 seconds for the nephrographic phase and approximately 5 min for the excretory phase). The arterial and delayed (excretory) images are obtained by scanning from the diaphragm through the symphysis pubis, while the nephrographic and non-contrast images are obtained by scanning from the diaphragm through the iliac crests. Longer delay for

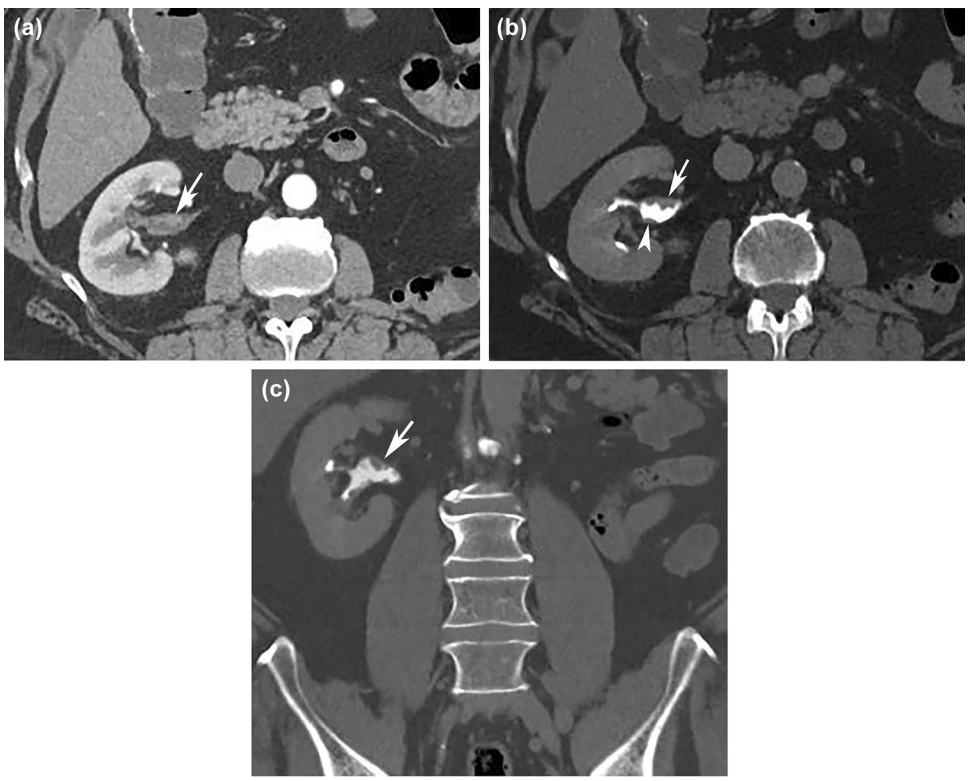

Fig. 3 Renal pelvis urothelial carcinoma. 66-year-old male with renal pelvis urothelial carcinoma. **a** Axial CT image of the right kidney in the arterial phase shows an enhancing lesion in the renal pelvis anteriorly (white arrow). **b** Axial CT image in the excretory phase (wide window setting), at the same level in (**a**), shows the lesion in (**a**) (white arrow) and additional lesion posteriorly which was not well seen on arterial phase image (white arrow head). **c** Multiple filling defects and irregularity of the renal pelvis are better seen on coronal CT image in the excretory phase (wide window setting)

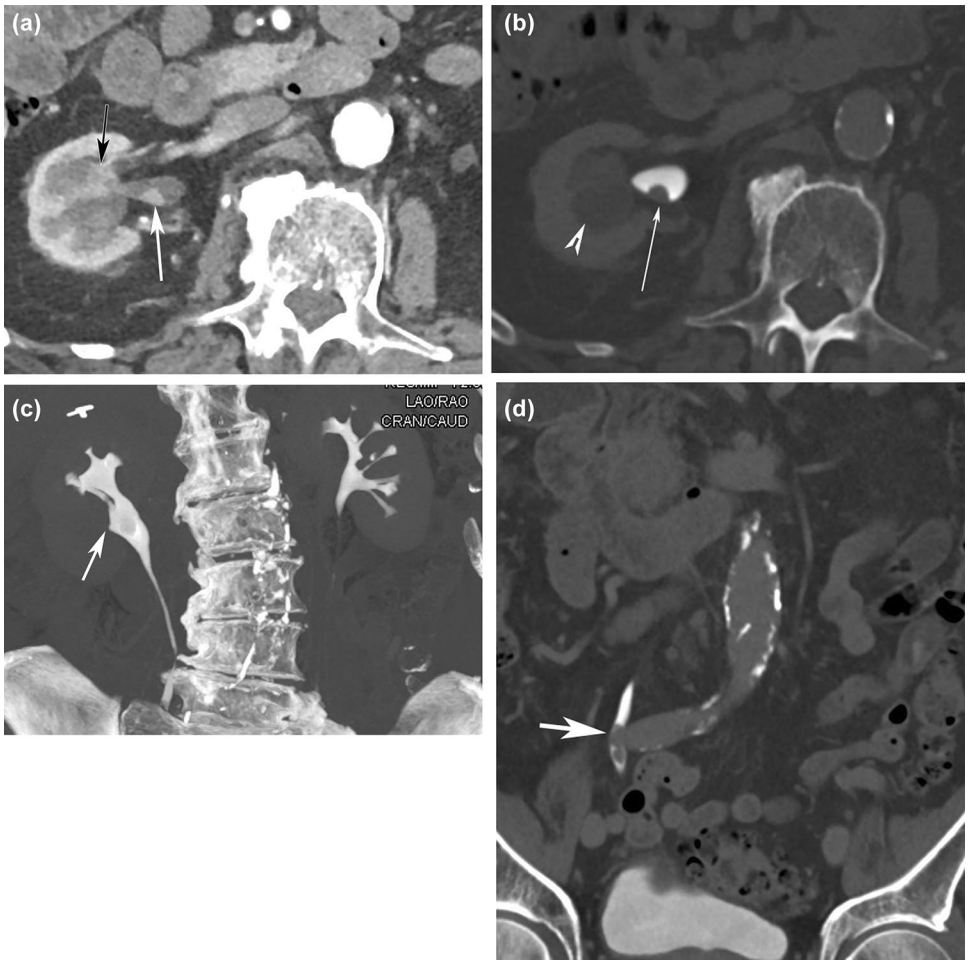

Fig. 4 Multifocal urothelial carcinoma. 90-year-old male with urothelial carcinoma. **a** Axial CT image of the abdomen in the arterial phase shows multiple-enhancing lesions in the lower pole calyx (black arrow) and avidly enhancing lesion in the renal pelvis (white arrow). **b** Axial CT image in the excretory phase show a filling defect in the renal pelvis (white arrow). Note the lack of contrast opacification of the lower pole calyces (white arrow head), which is better delineated on coronal MIP image in the excretory phase (white arrow) (**c**), a typical appearance of an amputated calyx. **d** Coronal CT image in the excretory phase at the level of the distal right ureter, shows a filling defect (white arrow), consistent with additional urothelial carcinoma

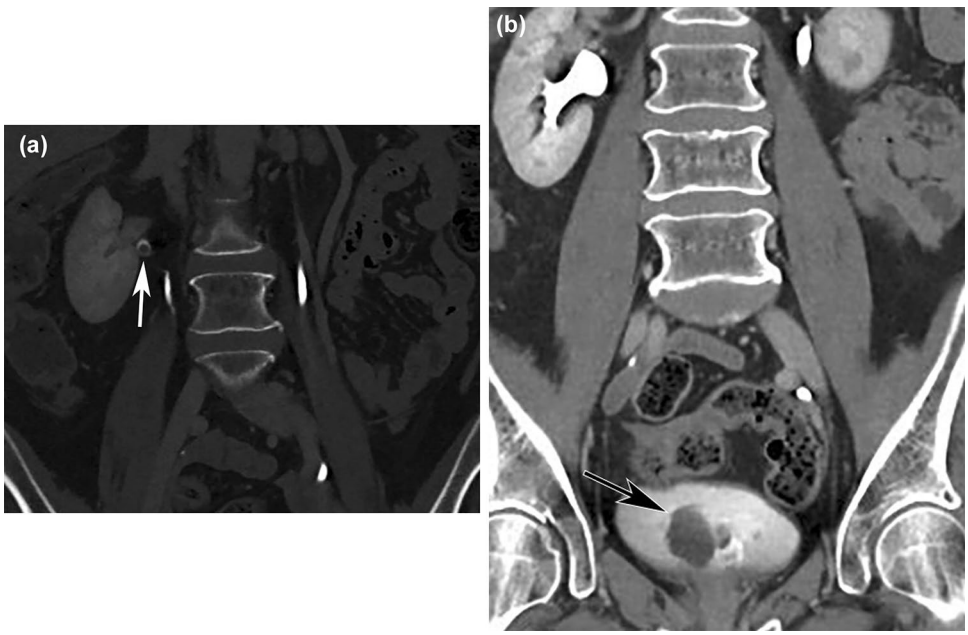

Fig. 5 Collecting system and urinary bladder blood clots. 67-year-old female with history of hematuria. **a** Coronal CT image of the abdomen in the excretory phase (wide window setting) shows a small filling defect in the right renal pelvis (white arrow). Note that the excreted contrast material completely surrounds the filling defect. **b** Coronal CT image of the abdomen and pelvis in the excretory phase shows a larger filling defect in the urinary bladder, which is also completely surrounded by excreted contrast material. The urine cytology was negative for atypical cells in this patient, and these filling defects were though to represent blood clots rather than malignancy

the excretory phase is typically avoided, as the increasing density of excreted contrast with time makes evaluation more challenging to see through the contrast to detect small lesions or areas of subtle urothelial thickening. Additionally, resultant beam-hardening artifact from dense excreted contrast material compromises the detection of lesions in the adjacent renal parenchyma [12, 21].

3D Imaging

Accurate diagnosis of UTT urothelial carcinoma requires careful evaluation of the source axial images in combination with multiplanar and 3D reconstructions. In fact, 3D reconstructions have become an integral part of CTU in recent years, as multidetector technology allows acquisition of isotropic source images. At our institution, the source axial images (0.5 mm) are sent to a separate workstation for creation of three sets of 3D reconstructions: maximum intensity projection (MIP), traditional volume-rendered reconstructions (VR), and virtual ureteroscopy images (specialized volume-rendered images) [24].

MIP images, arguably the most important reconstruction, allow for a global overview of the renal collecting system and ureters and better delineate subtle areas of urothelial thickening and strictures, especially at the junction of the

Fig. 6 Metachronous urothelial carcinoma in the ureter. 52-year-old female with history of prior right nephroureterectomy for urothelial carcinoma 10 years prior. **a** Axial CT image of the pelvis in the arterial phase, at the level of the distal left ureter, shows enhancing soft tissue in the ureter (white arrow). **b** Coronal CT image of the pelvis, at the same level in (**a**), shows a similar finding (white arrow). **c** Axial CT image of the pelvis in the excretory phase shows a filling defect in the distal left ureter (white arrow), which is also nicely seen on coronal excretory phase image at the same level (white arrow) (**d**). **e** Coronal MIP image in the excretory phase shows moderate left hydroureteronephrosis, with the transition point in the distal ureter, at the level of the soft tissue filling defect (white arrow)

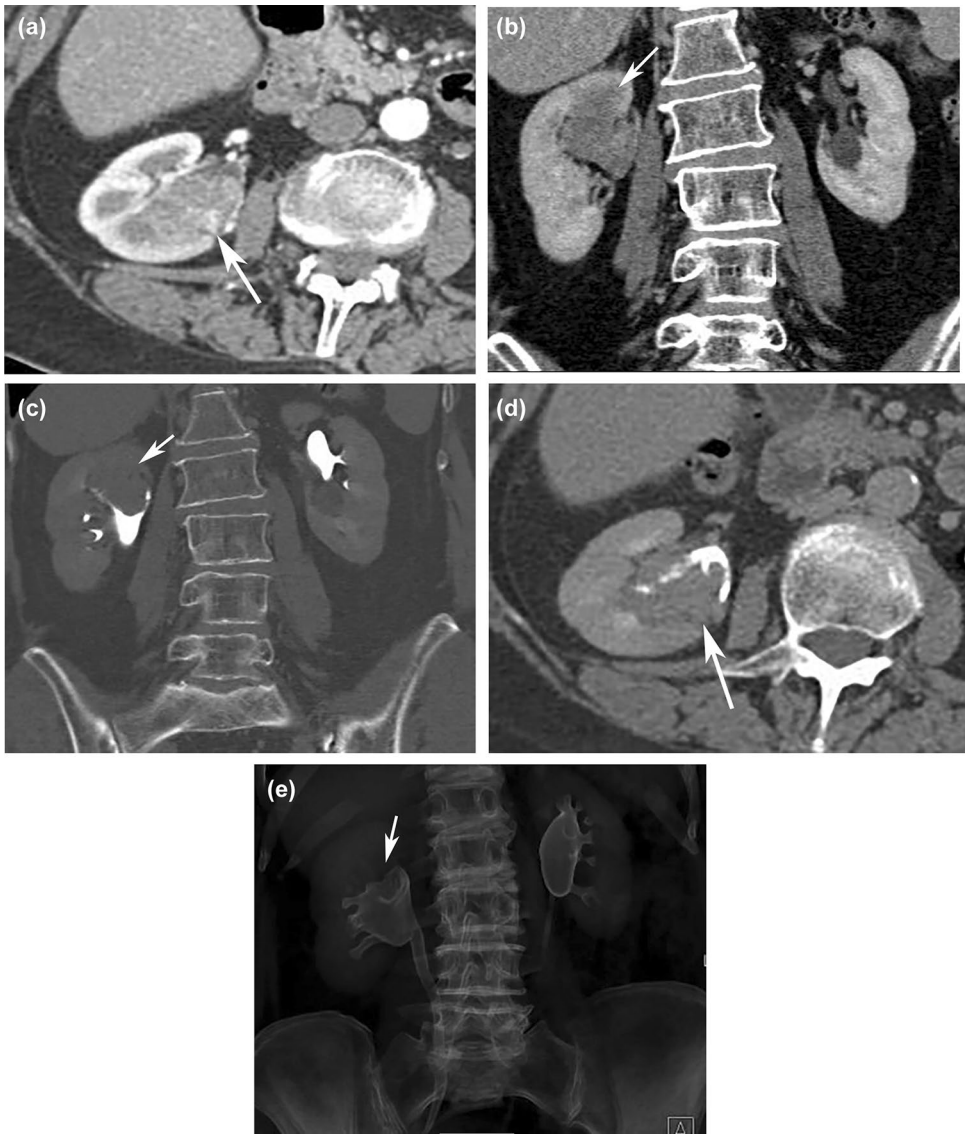

Fig. 7 Urothelial carcinoma with adjacent renal parenchymal involvement. 87-year-old female with history of urothelial carcinoma of the right kidney. **a** Axial CT image of the abdomen in the arterial phase shows enhancing soft tissue lesion in the upper pole collecting system (white arrow). Note the absence of fat plane between the soft tissue lesion and adjacent renal parenchyma. **b** Coronal CT image of the abdomen in the venous phase shows hypoattenuation in the renal parenchyma adjacent to the calyceal soft tissue lesion (white arrow), a finding that is concerning for contiguous involvement. **c** Coronal CT image of the abdomen in the excretory phase (wide window setting) demonstrates a large filling defect in the upper pole calyx of the right kidney, with extension into the renal pelvis (white arrow). **d** Axial CT image in the excretory phase shows the same finding in (**c**) (white arrow). **e** Obliteration of the upper pole calyx in the right kidney is nicely shown in this coronal volume-rendered reconstruction (white arrow). The patient had a pT3 tumor on surgical pathology

calyx and infundibulum, an area that is often difficult to evaluate on axial images, and can be easily overlooked. Six out of 27 urothelial carcinoma lesions reported by Caoili et al. [21] were detected only on 3D reconstructed images. One advantage of MIP images over standard two-dimensional (2D) images is the ability to view the entire ureter in one section. This helps accentuate areas of thickening, strictures, and subtle filling defects [24].

The collecting system can also be visualized from multiple views utilizing VR images. This technique is particularly helpful in delineating lesions in obstructed collecting systems, where minimal contrast is excreted [24]. Subtle areas of urothelial thickening can be missed with this technique, however [25].

Virtual ureteroscopy allows visualization of the collecting system in a translucent fashion. This technique is helpful in detection of subtle filling defects and areas of urothelial irregularity that can be obscured on MIP images due to surrounding dense contrast [24].

3D reconstructions, although a useful complementary tool in detection of subtle urothelial carcinomas, are susceptible to suboptimal distension of the collecting system and ureteral peristalsis, and both these limitations can be mistakenly interpreted as strictures. In addition, tumors producing soft tissue thickening without narrowing of the lumen are best demonstrated on the axial images [2]. Therefore, it is imperative to cross-reference the 3D images with axial source images to avoid these potential pitfalls [24].

Fig. 8 Infiltrative urothelial carcinoma in the kidney. 70-year-old female with history of infiltrative urothelial carcinoma of the left kidney. **a** Axial CT of the abdomen in the arterial phase shows significant soft tissue infiltration of the left kidney, with decreased perfusion. However, the renal contour is still preserved despite the marked infiltration, an imaging characteristic of infiltrative urothelial carcinoma. **b** Coronal CT image of the abdomen in the arterial phase shows similar finding. **c** Coronal CT image of the abdomen in the venous phase shows a filling defect in the left renal vein (white arrow), consistent with a thrombus (uncommon finding in urothelial carcinoma). **d** Axial CT image of the abdomen in the excretory phase (wide window setting) shows lack of contrast excretion in the collecting system in the left kidney compared to the right, secondary to extensive infiltration by urothelial carcinoma

CT imaging

Three imaging appearances of upper tract urothelial carcinoma have been described in the literature: focal urothelial thickening, focal intraluminal soft tissue mass or filling defect, and infiltrative mass. Published series of these uncommon lesions are small, hence it is difficult to ascertain which appearance is more common.

In one study by Caoili et al., the most common appearance was that of urothelial thickening [21]. Subtle urothelial thickening without associated urinary obstruction is notoriously difficult to detect. The problem is compounded by the fact that the distal ureter, a common location for ureteral urothelial carcinoma, is often underdistended, despite optimal technique. Small tumors of the ureter are often best visualized on the arterial phase as a focal area of enhancement and hypervascularity [21] or on 3D excretory MIP images. Some ureteral cancers do not cause significant luminal narrowing but are detected on the basis of focal ureteral wall thickening, which may be best depicted on the axial images (Fig. 1).

By contrast, small urothelial carcinoma of the upper collecting system blend with the adjacent unopacified renal medulla in the corticomedullary phase and are easier to detect as irregular areas of infundibular narrowing, focal amputation of a calyx or calyceal destruction in the excretory phase. Reviewing the images at wide windows and 3D imaging, especially MIP images, which offer a global view of the collecting system are especially useful [12] (Fig. 2).

Another appearance of upper tract urothelial carcinoma is that of a soft tissue mass, typically lower density than stones (except for indinavir stones). Small lesions ($\leq$ 5 mm) can be easily obscured by beam-hardening artifact from excreted contrast in the excretory phase images; using wide window settings to see through the dense intraluminal contrast, rather than the standard soft tissue window, is essential [21] (Fig. 3). Some small tumors enhance avidly and are thus are most conspicuous on the arterial or venous phase [23] (Fig. 4). Benign entities such as blood clots, sloughed papilla from papillary necrosis, or fungus balls also present as a filling defect in the collecting system. However, these mimickers tend to be completely intraluminal and surrounded with

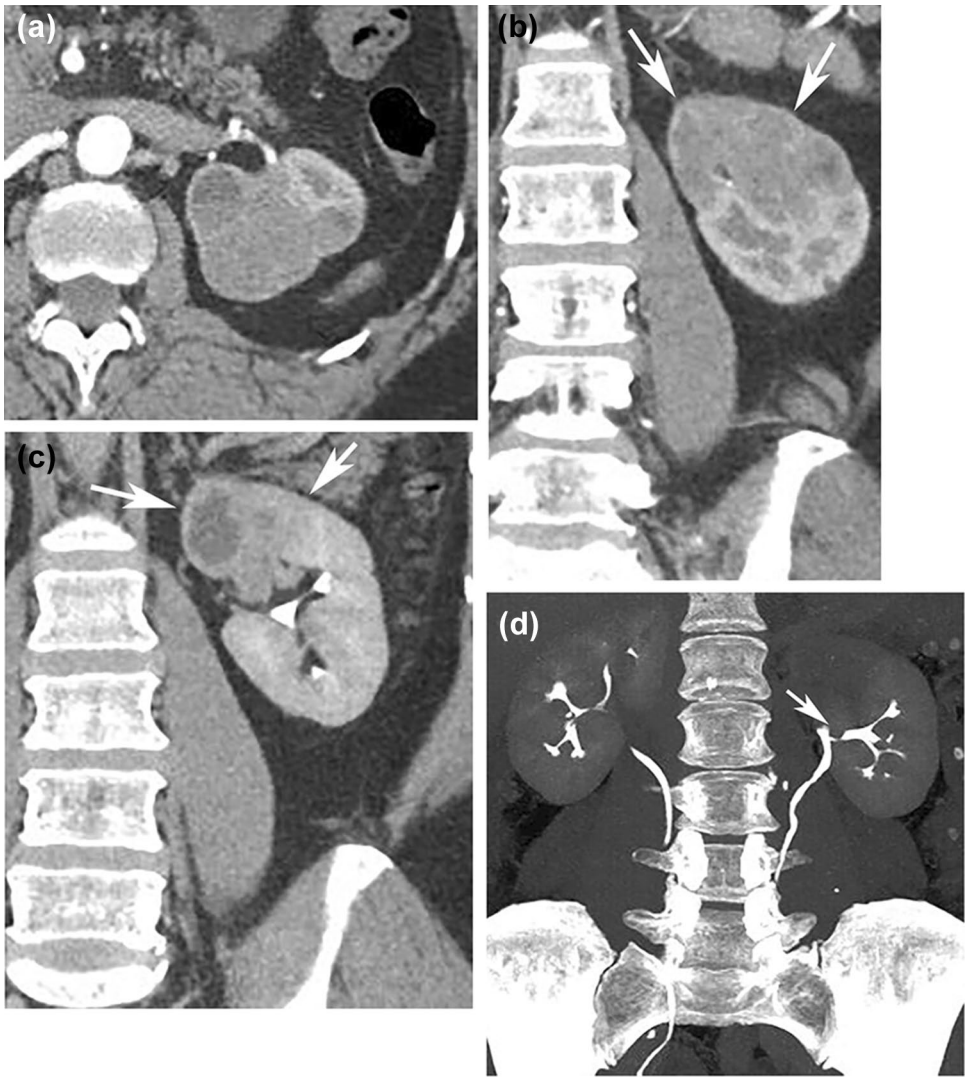

Fig. 9 Urothelial carcinoma with renal parenchymal involvement. 61-year-old female with history of urothelial carcinoma in the left kidney. **a** Axial CT image of the abdomen in the arterial phase shows ill-defined infiltration in the upper pole of the left kidney. **b** Coronal CT image of the abdomen in the arterial phase shows ill-defined infiltration in the upper portion of the left kidney. Note how the renal contour is still preserved (white arrows). **c** Coronal CT image in the excretory phase shows lack of contrast opacification in the upper pole collecting system and heterogeneous attenuation in the upper portion of the kidney (white arrows), consistent with renal parenchymal involvement. **d** Coronal MIP image in the excretory phase shows obliteration of the upper pole collecting system (amputated calyx) with soft tissue extension into the renal pelvis (white arrow). The patient had a pT3 tumor on surgical pathology

Table 1 TNM staging of upper urinary tract TCC [4]

TNM stage	Disease extent
Ta	Noninvasive papillary carcinoma that is confined to urothelium and projecting toward the lumen
Tis	Carcinoma in situ: flat tumor with high-grade histologic features that is confined to urothelium
T1	Tumor invades subepithelial connective tissue (lamina propria)
T2	Tumor invades muscularis
T3	Renal pelvis: Tumor invades beyond the muscularis into the peripelvic fat or renal parenchyma
T4	Tumor invades adjacent organs, the pelvic or abdominal wall, or through the kidney into the perinephric fat
N0	No regional lymph node metastasis
N1	Metastasis to a single lymph node that is < 2 cm in greatest dimension
N2	Metastasis to a lymph node that is 2–5 cm in greatest dimension or to multiple lymph nodes, none of which is > 5 cm in greatest dimension
N3	Metastasis to a lymph node that is > 5 cm in greatest dimension
M0	No distant metastasis
M1	Distant metastasis

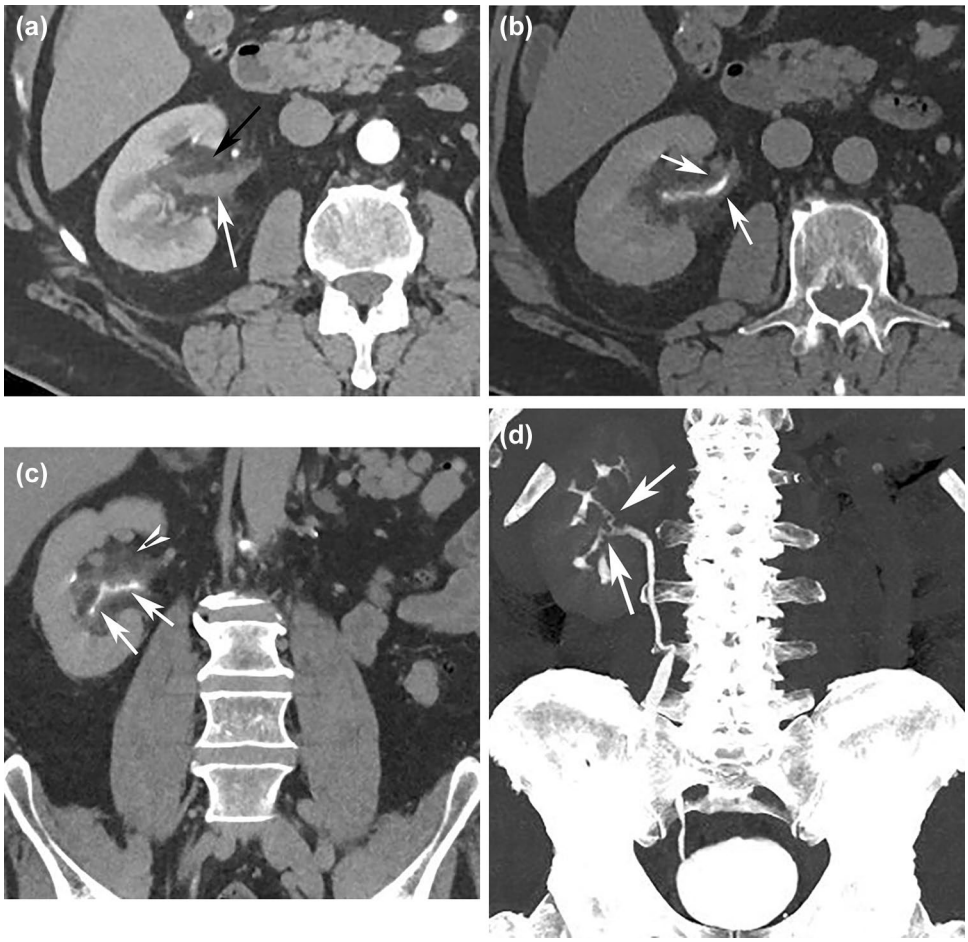

Fig. 10 Urothelial carcinoma with extension beyond the muscularis. 66-year-old male with history of urothelial carcinoma of the right kidney. **a** Axial CT image of the abdomen in the arterial phase shows enhancing soft tissue in the right renal pelvis (white arrow) with haziness in the surrounding fat (black arrow). **b** Axial CT image in the excretory phase better delineates the urothelial thickening in the renal pelvis (white arrows). **c** Coronal image in the excretory phase (wide window setting) shows extensive urothelial thickening in the renal pelvis and lower pole collecting system (white arrows). Haziness of the surrounding fat is also shown (white arrowhead), a suspicious finding for extension beyond the muscularis. **d** Coronal MIP image in the excretory phase nicely demonstrates wall irregularity in the collecting system (white arrows)

excreted contrast on delayed phase images. Additionally, these do not enhance on post-contrast images [26] (Fig. 5).

Some upper tract urothelial carcinoma present as a locally aggressive, infiltrative mass distorting or obstructing the renal collecting system or ureter, and causing upstream dilatation [2] (Fig. 6). Infiltration into adjacent renal parenchyma is suggested by hypoenhancement of the renal parenchyma with heterogeneous attenuation [27] (Fig. 7). However, the reniform shape of the kidney tends to be preserved in contrast to contour expansion seen with renal cell carcinoma [4, 5] (Fig. 8). Identification of renal parenchymal invasion is a crucial imaging finding, as this will help differentiate early-stage (I and II) from advanced-stage tumors (III and IV) (Fig. 9). When upper tract urothelial carcinoma infiltrate the kidney, aggressive forms of renal cell carcinoma (such as duct of Bellini or medullary cancer), lymphoma, or metastases are among the main diagnostic considerations. Bacterial pyelonephritis, which can also have a similar appearance, is usually diagnosed clinically [26].

Calcifications are uncommon. Linear or punctate incrustations within an irregular soft tissue mass or thickening allows differentiation from a chronic inflammatory process.

Urothelial tumors do obstruct the collecting system and present with stricture of an infundibulum with focal calyceal dilatation or destruction. Careful assessment for subtle hydronephrosis or hydroureter or asymmetry in ureteral distension may be the first indication of the small ureteral tumor. The area of transition between the dilated portion and the normal caliber ureter should be carefully inspected for the presence of a lesion (Fig. 1). Rarely, slow-growing tumors cause long-standing obstruction resulting in a hydronephrotic sac with thin, poorly or nonfunctioning renal parenchyma [28].

Staging

The TNM system is the most frequently used for staging [4] (Table 1). Initial staging is crucial in dictating future management and prediction of prognosis. When urothelial carcinoma involves the renal collecting system, if a fat plane or a layer of excreted contrast material is present between the mass and renal parenchyma, the tumor is classified as T1 or T2 [4]. Stage T3 tumors extend beyond the muscularis into the adjacent peripelvic fat or renal

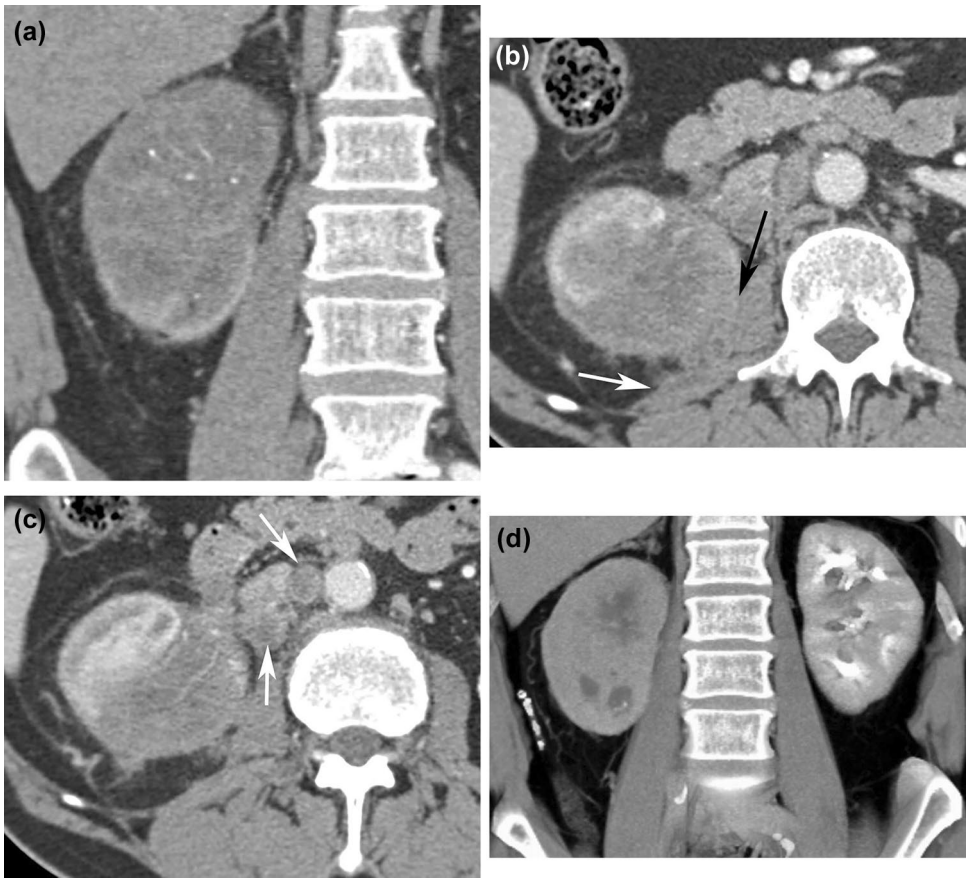

Fig. 11 Infiltrative urothelial carcinoma with extra-renal extension. 61-year-old male with urothelial carcinoma of the right kidney. **a** Coronal CT image of the abdomen in the arterial phase shows diffuse infiltration of the right kidney with poor perfusion. Note how the renal contour is preserved despite the extensive soft tissue infiltration. **b** Axial CT image in the venous phase shows the same finding in (**a**). Note the loss of fat plane between the kidney and the right psoas muscle (black arrow). Loss of intervening fat plane with the quadratus lumborum muscle is also noted with heterogeneous attenuation of the muscle (white arrow); these findings are highly suggestive of local extension of malignancy. **c** Axial CT image in the venous phase shows enlarged and hypoattenuating retroperitoneal lymph nodes, which are likely metastatic. **d** Coronal 3D reconstruction in the excretory phase shows complete lack of opacification of the right renal collecting system compared to the left, secondary to infiltration by malignancy

parenchyma. Obliteration of renal sinus fat or abnormal enhancement in the adjacent renal parenchyma is, therefore, typically seen (Fig. 10). Invasion through the kidney into the perinephric fat or adjacent organs is a sign of stage T4 tumors (Fig. 11).

The ability to predict tumor stage has important management and prognostic implications. In one study of 39 consecutive patients, Fritz and colleagues achieved an accuracy of 87.8% [29]. In their series, understaging due to microscopic peri tumoral invasion at pathology was more common than overstaging caused by inflammatory changes. Some benign entities such as infection, hemorrhage, or inflammation may mistakenly be interpreted as a higher pathologic stage. Furthermore, delayed cortical nephrogram, one of the signs suggestive of parenchymal invasion, is also seen in pyelonephritis, obstructive uropathy, or renal vascular disease [26].

Summary

Urothelial carcinoma of the upper urinary tract is a relatively uncommon malignancy. Multifocality and high rates of recurrence are key features of these tumors. The CTU protocol focuses on maximizing ureteral distension to optimize detection of small lesions in the collecting system. 3D imaging helps maximize sensitivity of CTU in detection of subtle tumors. CTU tends to perform well in differentiating early stage from advanced-stage tumors; however, it is not that accurate in differentiation among early-stage tumors (Ta, T1, and T2).

References

1. Chlapoutakis K, et al. (2010) *Performance of computed tomographic urography in diagnosis of upper urinary tract urothelial carcinoma, in patients presenting with hematuria: Systematic review and meta-analysis*. Eur J Radiol **73**(2):334–8
2. Caoili EM, Cohan RH (2016) *CT urography in evaluation of urothelial tumors of the kidney*. Abdom Radiol (NY) **41**(6):1100–7
3. Kirkali Z, Tuzel E (2003) *Transitional cell carcinoma of the ureter and renal pelvis*. Crit Rev Oncol Hematol **47**(2):155–69
4. Vikram R, Sandler CM, Ng CS (2009) *Imaging and staging of transitional cell carcinoma: part 2, upper urinary tract*. AJR Am J Roentgenol **192**(6):1488–93
5. Browne RF, et al. (2005) *Transitional cell carcinoma of the upper urinary tract: spectrum of imaging findings*. Radiographics **25**(6):1609–27
6. Polenakovic M, Stefanovic V (2014) *What do we know about the Balkan endemic nephropathy and the uroepithelial tumors?*. Pril (Makedon Akad Nauk Umet Odd Med Nauki) **35**(1):11–15
7. Buckley JA, et al. (1996) *Transitional cell carcinoma of the renal pelvis: a retrospective look at CT staging with pathologic correlation*. Radiology **201**(1):194–8
8. Davis R, et al. (2012) *Diagnosis, evaluation and follow-up of asymptomatic microhematuria (AMH) in adults: AUA guideline*. J Urol **188**(6 Suppl):2473–2481
9. Jinzaki M, et al. (2011) *Comparison of CT urography and excretory urography in the detection and localization of urothelial carcinoma of the upper urinary tract*. AJR Am J Roentgenol **196**(5):1102–9
10. Sudakoff, G.S., et al., *Multidetector computerized tomography urography as the primary imaging modality for detecting urinary tract neoplasms in patients with asymptomatic hematuria.* J Urol, 2008. **179**(3): p. 862-7; discussion 867.
11. Sadow CA, et al. (2010) *Positive predictive value of CT urography in the evaluation of upper tract urothelial cancer*. AJR Am J Roentgenol **195**(5):W337–43
12. Raman SP, Fishman EK (2018) *Upper and Lower Tract Urothelial Imaging Using Computed Tomography Urography*. Urol Clin North Am **45**(3):389–405
13. Takeuchi M, et al. (2012) *Split-bolus CT-urography using dual-energy CT: feasibility, image quality and dose reduction*. Eur J Radiol **81**(11):3160–5
14. Chen CY, et al. (2016) *Diagnostic Performance of Split-Bolus Portal Venous Phase Dual-Energy CT Urography in Patients With Hematuria*. AJR Am J Roentgenol **206**(5):1013–22
15. Kaza RK, Platt JF (2016) *Renal applications of dual-energy CT*. Abdom Radiol (NY) **41**(6):1122–32
16. Dillman JR, et al. (2007) *Comparison of urinary tract distension and opacification using single-bolus 3-Phase vs split-bolus 2-phase multidetector row CT urography*. J Comput Assist Tomogr **31**(5):750–7
17. Chow LC, et al. (2007) *Split-bolus MDCT urography with synchronous nephrographic and excretory phase enhancement*. AJR Am J Roentgenol **189**(2):314–22
18. McTavish JD, et al. (2002) *Multi-detector row CT urography: comparison of strategies for depicting the normal urinary collecting system*. Radiology **225**(3):783–90
19. Silverman SG, et al. (2006) *Multi-detector row CT urography of normal urinary collecting system: furosemide versus saline as adjunct to contrast medium*. Radiology **240**(3):749–55
20. Sanyal R, et al. (2007) *CT urography: a comparison of strategies for upper urinary tract opacification*. Eur Radiol **17**(5):1262–6
21. Caoili EM, et al. (2005) *MDCT urography of upper tract urothelial neoplasms*. AJR Am J Roentgenol **184**(6):1873–81
22. Raman SP, Fishman EK (2014) *Bladder malignancies on CT: the underrated role of CT in diagnosis*. AJR Am J Roentgenol **203**(2):347–54
23. Raman SP, Horton KM, Fishman EK (2013) *MDCT evaluation of ureteral tumors: advantages of 3D reconstruction and volume visualization*. AJR Am J Roentgenol **201**(6):1239–47
24. Raman SP, Horton KM, Fishman EK (2012) *Transitional cell carcinoma of the upper urinary tract: optimizing image interpretation with 3D reconstructions*. Abdom Imaging **37**(6):1129–40
25. Washburn ZW, et al. (2009) *Computed tomographic urography update: an evolving urinary tract imaging modality*. Semin Ultrasound CT MR **30**(4):233–45
26. Kawamoto S, Horton KM, Fishman EK (2008) *Transitional cell neoplasm of the upper urinary tract: evaluation with MDCT*. AJR Am J Roentgenol **191**(2):416–22
27. Hartman DS, et al. (1988) *Infiltrative renal lesions: CT-sonographic-pathologic correlation*. AJR Am J Roentgenol **150**(5):1061–4
28. Prando A, Prando P, Prando D (2010) *Urothelial cancer of the renal pelvicaliceal system: unusual imaging manifestations*. Radiographics **30**(6):1553–66
29. Fritz GA, et al. (2006) *Multiphasic multidetector-row CT (MDCT) in detection and staging of transitional cell carcinomas of the upper urinary tract*. Eur Radiol **16**(6):1244–52